HHS Public Access

Author manuscript

J Immunol. Author manuscript; available in PMC 2021 February 15.

Published in final edited form as:

J Immunol. 2020 February 15; 204(4): 980–989. doi:10.4049/jimmunol.1900639.

Neonatal injury increases gut permeability by epigenetically suppressing E-cadherin in adulthood

Kevin T. Kline[1,*], **Haifeng Lian**[1,2,*], **Xiaoying S. Zhong**[1], **Xiuju Luo**[3], **John H. Winston**[1], **Yingzi Cong**[4], **Tor C. Savidge**[5], **Roderick H. Dashwood**[6], **Don W. Powell**[1], **Qingjie Li**[1]

[1]Division of Gastroenterology, Dept. of Internal Medicine, The University of Texas Medical Branch at Galveston, Galveston, TX

[2]Dept. of Gastroenterology, Binzhou Medical University Hospital, Binzhou, China

[3]Dept. of Laboratory Medicine, Xiangya School of Medicine, Central South University, Changsha, China

[4]Dept. of Microbiology and Immunology, The University of Texas Medical Branch at Galveston, Galveston, TX

[5]Texas Children's Microbiome Center, Baylor College of Medicine, Houston, TX

[6]Center for Epigenetics & Disease Prevention, Texas A&M College of Medicine, Houston, TX

Abstract

Altered intestinal epithelial integrity is an important susceptibility trait in inflammatory bowel disease (IBD) and early life stressors are reported to contribute to this disease susceptibility in adulthood. To identify disease mechanisms associated with early life trauma that exacerbate IBD in adulthood we used a ‘double-hit’ neonatal (NI) and adult inflammation (AI) model that exhibits more severe mucosal injury in the colon later in life. Herein, we explore the underlying mechanisms of this aggravated injury. In rats exposed to both NI and AI, we found sustained increases in colonic permeability accompanied by significantly attenuated expression of the epithelial junction protein E-cadherin. Quantitative RT-PCR revealed a decreased *Cdh1* (gene of E-cadherin) mRNA expression in NI+AI rats compared to NI or AI rats. Next, we performed miRNA microarrays to identify potential regulators of E-cadherin in NI+AI rats. We confirmed the overexpression of miR-155, a predicted regulator of E-cadherin, and selected it for further analysis based on reported significance in human IBD. Using ingenuity pathway analysis software, the targets and related canonical pathway of miR-155 were analyzed. Mechanistic studies identified histone hyperacetylation at the Mir155 promoter in NI+AI rats, concomitant with elevated RNA polymerase II binding. In vitro, E-cadherin knockdown markedly increased epithelial cell permeability, as did overexpression of miR-155 mimics which significantly suppressed E-cadherin protein. In vivo, NI+AI colonic permeability was significantly reversed with administration of miR-155 inhibitor rectally. Our collective findings indicate that early life inflammatory stressors

Corresponding Author: Qingjie Li, PhD, Associate Professor, Division of Gastroenterology, Department of Internal Medicine, The University of Texas Medical Branch at Galveston, 301 University Boulevard, Galveston, Texas 77555-1074, USA. quli@utmb.edu.

*K.T.K. and H.L. contributed equally as first authors.

trigger a significant and sustained epithelial injury by suppressing E-cadherin through epigenetic mechanisms.

Keywords

Early life adversity; E-cadherin; epigenetics; intestinal epithelial barrier; microRNA-155

INTRODUCTION

The integrity of the epithelial cell junction barrier of the intestines is thought to play an essential role in the mediation of inflammation and disease pathogenesis (1). This has been well studied in inflammatory bowel disease (IBD), a group of conditions associated with chronic inflammation of the gastrointestinal tract. Tight and adherens junction proteins have been implicated in the pathogenesis of IBD. This includes E-cadherin, an essential adherens junction protein that is also required for tight junction formation (2). Alterations of E-cadherin structure and down-regulation of production promote a pro-inflammatory state, in part, by facilitating the transmigration of neutrophils (3, 4) and by serving as the binding ligand for the intestinal epithelial lymphocyte homing receptor α^E, which is a critical regulator of immune homeostasis in the intestine (5, 6).

Besides structural changes, the prolonged, vacillating immune response characteristic of IBD is thought to be mediated by varied mechanisms. One area of investigation has been perinatal stress, and the predisposition to diseases later in life, including IBD. We have previously demonstrated in rats that episodes of neonatal inflammation create epigenetic changes, leading to an exaggerated immune response when exposed to a second stress later in life (7). This response was associated with an increase in IL-1β production after an episode of adult inflammation (AI), but was dependent on the precedent-setting neonatal inflammation (NI). The exaggerated immune response after NI appeared to be mediated in part by epigenetic changes: specifically, the acetylation around NF-κB binding motifs leading to exaggerated IL-1β activation following an episode of AI. Importantly, adult rats given multiple inflammatory insults did not generate this aggravated IL-1β response, reinforcing the neonatal period as a critical determinant of the aggravated chronic inflammatory changes.

Within this dual inflammatory event model, the specific role of miRNA remains unclear. MicroRNAs play an important role in a variety of developmental processes and diseases by modulating gene expression through their interaction with mRNA targets, which inhibits translation and/or degrades mRNA. Despite the inherent limitations of *in silico* prediction tools and the difficulty in determining direct *vs.* indirect consequences of miRNA interactions, promising discoveries have come from such approaches in the study of IBD (8). Circulating miRNA with differential expression in ulcerative colitis (UC) and Crohn's disease (CD) have been proposed as biomarkers to distinguish between the two IBD subtypes (9). Changes in miRNA expression and the interaction with canonical pathways associated with IBD have previously been noted (10). Specifically, bioinformatics analysis has demonstrated or predicted multiple miRNAs that target E-cadherin, including miR-155.

MiR-155 plays an important role in various aspects of normal immune function; alterations in miR-155 expression and its association with IBD has been well established (11). Compared to healthy controls, patients with UC have a significant increase in miR-155 levels both in the circulation (9) and in colonic mucosa (12). MiR-155 is an important mediator of T-cell regulated immunity, and is required to induce Th17 driven chronic colitis in mice (13, 14). This is noteworthy, because E-cadherin sensitized dendritic cells also have been shown to increase Th17 driven immune responses and colitis (15).

We hypothesized that our novel model of exaggerated immune response, triggered by NI, was mediated by a change in intestinal permeability. We postulated that changes in epithelial integrity would be accompanied by a decrease in the expression of junction proteins. In addition, we hypothesized that the changes, in part, would be mediated by specific miRNAs that interact with target mRNAs of critical junction proteins in the gut. The current work reinforces our previous findings of NI increasing susceptibility to aggravated inflammation when a second stressor is provided. These changes were initiated by increased colonic permeability, corresponding to a significant decrease in the expression of E-cadherin and mediated, at least in part, by miR-155.

MATERIALS AND METHODS

Reagents.

Fluorescein isothiocyanate (FITC)–dextran (MW 4,000), 2,4,6-trinitrobenzene sulfonic acid (TNBS), and lipopolysaccharide (LPS) were purchased from Sigma (St. Louis, MO). Human tumor necrosis factor alpha (TNFα) and interleukin-1 beta (IL-1β) were purchased from Genscript (Piscataway, NJ).

Cell culture and in vitro permeability assay.

Caco-2, SW620, CCD 841 CoN and HEK293 cells purchased from ATCC (Manassas, VA) were maintained in DMEM medium supplemented with 10% FBS and 0.1% penicillin-streptomycin solution. Transient transfection was performed using Lipofectamine RNAiMAX (Thermo Fisher Scientific, Waltham, MA). To measure epithelial monolayer permeability, confluent epithelial cell monolayers, cultured on a permeable surface, were placed in a cell culture plate to form donor-receiver compartments (16) . FITC-dextran test compounds are added to the apical compartment, with fresh medium in the basolateral compartment. The transport of FITC-dextran across the epithelial cell monolayer was monitored.

Animals and procedures.

Male Sprague Dawley (SD) rat littermates were used in the preclinical studies. Five-day old pups were purchased from Envigo (Houston, TX). The procedures were approved by the Institutional Animal Care and Use Committee, The University of Texas Medical Branch at Galveston.

Rat neonates were randomly divided into four groups: 1) vehicle treatment in both neonatal and adult-life stages (Ctl+Ctl); 2) sham treatment as neonates followed by an inflammatory

insult as adults (Ctl+AI); 3) NI and then sham treatment as adults (NI+Ctl); and 4) NI plus AI in combination (NI+AI) (Fig. 1A). Experimenters were blinded to treatment assignment. To induce NI, TNBS (130 mg/kg dissolved in 200 μl saline containing 10% ethanol, a concentration previously established to ensure neonatal viability) was injected intraluminally 2 cm into the colon of pups on postnatal day 10 (17, 18) . The animals were kept in a head-down position while the anus was held closed for one minute to prevent leakage. Rats in the sham treatment groups received 200 μl of saline. In an interval necessary to induce significant change, six to eight weeks later, animals were subjected to a secondary TNBS (68 mg/kg) insult, as AI. Under light anesthesia, 250 μl of TNBS in PBS containing 40% ethanol was injected intrarectally via a catheter, advanced to 8 cm into the colon. Control rats were given 250 μl of saline. Epithelial permeability in the colon was assessed 7, 14, or 28 days after the second TNBS treatment. To determine whether a delayed first-time AI also aggravates the immune response, comparable to NI treatment, we also induced AI with TNBS (130 mg/kg) in 6- to 8-week old rats followed by a second AI (68 mg/kg TNBS) 6 weeks later (4 groups: Ctl+Ctl, Ctl+AI, AI+Ctl, and AI+AI). One week after the second TNBS administration, epithelial permeability in the colon was determined.

To assess colonic permeability, animals were fasted overnight with free access to GoLitely (Braintree Laboratories, Braintree, MA). Under light anesthesia with isoflurane, FITC-dextran dissolved in PBS (40 mg/ml, 200 μl) was administered intraluminally via catheter into the colon. Two hours later, animals were euthanized and blood collected for serum fluorescein measurement. For histologic examination, a full-thickness colon specimen was obtained from the proximal, middle and distal colon, fixed in 10% formalin, embedded in paraffin, sectioned, and stained with hematoxylin and eosin (H&E) (42). Immune cells (neutrophils, leukocytes, B and T lymphocytes, and mast cells) were stained and evaluated by two independent pathologists in a blinded manner. The mucosa/submucosa layers were dissected from the rest of the colon, snap-frozen in liquid nitrogen, pulverized, and stored at −80 °C for molecular studies.

Treatment of NI+AI rats with miR-155 inhibitor.

Ctl+Ctl and NI+AI rats were used for miR-155 inhibitor treatment. Both groups of rats were treated with either miRCURY LNA miRNA Inhibitor control (Cat. No. YI00199006) or rno-miR-155-5p miRCURY LNA miRNA inhibitor (Cat. No. YI0401318) via enema (10 nm in 200 μl PBS per injection), once daily from one day before through 6 days after the AI (19, 20). Colonic permeability was assessed 24 hours after the last dose of treatment. The mucosa/submucosa layers were dissected from the distal colon and used for detection of mRNA and protein by RT-qPCR and Western blot, respectively.

Quantitative RT-PCR (RT-qPCR).

Total RNA containing miRNA was extracted using the miRNeasy Mini Kit (QIAGEN, Valencia, CA), followed by cDNA synthesis using SuperScript III First-Strand Synthesis System or TaqMan™ Advanced miRNA cDNA Synthesis Kit (Invitrogen). The mRNA and miRNA levels were quantitated using TaqMan-based qPCR, with18S *rRNA* and *U6 snRNA* as internal controls, respectively.

Quantitative methylation-specific PCR (qMSP).

Genomic DNA was extracted using DNeasy Blood & Tissue Kit (QIAGEN), followed by sodium bisulfite conversion using EpiMark Bisulfite Conversion Kit (NEB, Ipswich, MA). SYBR green-based qMSP with primers specific to the methylated rat *Mir155* promoter (Rt-Mir155-M-F: 5'-gtc ttg gga gct ttt aca gtg g-3'; Rt-Mir155-M-R: 5'-ggc cac cac ctc cta gca a-3') was performed in a QuantStudio 6 Flex Real-Time PCR System (Thermo Fisher). Primers specific to the rat *Mmp9* promoter (Mmp9-MSP-F: 5'-tga ggt tgg gaa atg gtg gac-3'; Mmp9-MSP-R: 5'-tgt aca gac ctg tga gac gg-3') were included as internal control.

Immunoblotting.

Western blotting was performed as described previously (7). Primary antibodies were as follows: Anti-E-cadherin (Cat. # AF648, R&D Systems, 1:1000), anti-β-Actin mouse monoclonal antibody (Cat. # A5441, Sigma, 1:5000), anti-β-catenin (A11343), Claudin 1 (A2196), Claudin 2 (A14085), Caludin 8 (A8174) and Occludin (A2601) rabbit polyclonal antibodies (ABclonal, Woburn, MA), and anti-Claudin 1 (bs-8482R) and Claudin 15 (bs-13753) rabbit polyclonal antibodies (Bioss Antibodies, Woburn, MA). All blots were scanned using an Odyssey Infrared Imaging System (LI-COR Biosciences, Lincoln, Nebraska). Band density was determined using LI-COR Image Studio Software.

Immunohistochemistry.

Full-thickness colon tissue was fixed in 10% formalin and embedded in paraffin. Ten-micrometer sections were baked in a 50-55 °C oven for 1 hour. After antigen retrieval and one-hour blocking with 10% serum, the slides were treated with anti-E-cadherin mouse monoclonal antibody (sc-71007, Santa Cruz Biotechnology; 1:50 dilution) overnight, followed by washing three times 15 min each with 1X PBS. The sections were then incubated for 1 hour at room temperature with ALEXA-conjugated antibody (Invitrogen) diluted 1:400 in PBS. Images were captured using a LEICA DMI 6000 B microscope.

MicroRNA microarrays.

MicroRNA microarrays were performed by LC Sciences (Houston, TX) using Microarray Version 21 (MRA-1003). Data were analyzed by subtracting the background and then normalizing the signals using a LOWESS (Locally-Weighted Regression) filter. The miRNA transcript was considered as reliably detectable only if the signal intensity was greater than 3 times the background standard deviation; the spot coefficient of variation was < 0.5, and at least 50% of the repeated probe signals were above the detection level.

MicroRNA Targets Prediction and Ingenuity Pathway Analysis (IPA).

Utilizing IPA (Ingenuity Pathway Analysis, Redwood, CA) software, miRNAs of interest were imputed and cross-referenced with described TargetScan human targets. Using the biomarker dataset upload, the ingenuity identifier was selected, and an overlay of the tight junction canonical pathway was implemented.

Chromatin immunoprecipitation (ChIP).

ChIP assays were performed as described previously using ChIP-IT Express kit (Active Motif, Carlsbad, CA) (42). Antibodies for the immunoprecipitation are as follows: Histone H3 acetyl Lysine 9 (H3K9ac, Cat. # 39137), histone H4 acetyl Lysine 12 (H4K12ac, Cat. # 39165), and RNA polymerase II (Cat. # 39097, Active Motif, Carlsbad, CA). Precipitated DNA, PowerUp™ SYBR™ Green Master Mix (Applied Biosystems, Foster City, CA), and primers specific to the rat *Mir155* gene promoter (forward: 5'-ggc ttg ctg aag gct gta tg-3', reverse: 5'-aca ggt agg agt cag tca gag g-3') were used for real-time polymerase chain reaction (qPCR). Fold differences in precipitated DNA were normalized against input.

Statistics.

All data were expressed as mean ± SD. We used one-way analysis of variance (ANOVA) followed by Tukey post-hoc analysis for comparison of more than two means, and Student's t-test to compare between two means, and considered $P<0.05$ to be statistically significant.

RESULTS

NI+AI aggravated mucosal injury leads to increased intestinal permeability.

First, to evaluate the effect of NI and AI on colonic epithelial integrity we assessed the intestinal permeability in all four groups of male rats at an interval of 7, 14, and 28 days from the adult inflammatory insult (TNBS) administered at 8 weeks (Fig. 1A). Permeability was significantly increased in NI+AI rats compared to Ctl+AI at all intervals, *i.e.*, Days 7, 14 and 28 (Figs. 1B-D, $P<0.05$). These changes in permeability accompanied increased architectural distortion and epithelial damage, as viewed in H&E stained colonic specimens of NI+AI rats compared to other groups (Fig. 1E). There was a significant, pan-colonic infiltration of neutrophils in NI+AI group *vs.* the other three groups (Figs. 1F-H, $P<0.01$). These findings were mirrored in an NI+AI dependent manner in other immune cells known to influence epithelial barrier function: leukocytes, B and T lymphocytes, and mast cells (Fig. S1). A small, but statistically significant increase in permeability occurred in Ctl+AI rats at day 7 but was not sustained at later time-points. This corresponded with an increase in colonic neutrophils. When comparing neutrophil infiltration between groups the NI+AI was significantly increased compared to the Ctl+AI in all areas of the colon (Figs. 1F-H, $P<0.01$). There was no significant difference in permeability among NI+Ctl rats compared to the Ctl+Ctl groups (Figs. 1B-D). These findings suggest that the combination of NI and AI is necessary to create a significant and sustained increase in permeability, and that a single insult later in life will not reproduce the exacerbated response triggered by an initial NI episode.

At 7 days, we also evaluated adult rats that were exposed to two rounds of AI, and there was a significant increase in permeability noted in Ctl+AI and AI+AI as compared to Ctl+Ctl ($P<0.05$), but no significant change between Ctl+AI and AI+AI ($P>0.05$)(Fig. 1I). These findings were accompanied by a significant increase in neutrophil concentration in Ctl+AI and AI+AI groups compared to Ctl+Ctl ($P<0.05$), with again no significant change between the increased groups ($P>0.05$) (Figs. 1J-L). Neither the change in permeability nor neutrophil concentration was as sizable as that seen after a neonatal insult. These findings

support our previous findings that multiple AI episodes, later in life, fail to recapitulate the NI+AI paradigm, and do not significantly change intestinal permeability in the absence of NI (7).

NI+AI exacerbates decreased E-cadherin expression.

To elucidate the molecular mechanisms underlying the increase of colonic permeability in NI+AI rats, we compared the expression levels of junction proteins in colonic mucosa/submucosa. Protein levels of β-catenin, claudin 1, claudin 2, claudin 7, claudin 8, claudin 15, and occludin remained the same in all 4 groups of rats (Fig. S2). However, E-cadherin protein levels were markedly attenuated in the colonic mucosa/submucosa of NI+AI compared to the other three groups of rats ($P<0.05$) (Fig. 2A). Immunofluorescence staining corroborated the decreased intensity of E-cadherin expression in NI+AI rats (Fig. 2B). When evaluating E-cadherin protein expression in adult rats subjected to two rounds of AI, there was no significant difference between Ctl+Ctl, Ctl+AI, AI+Ctl, and AI+AI groups (Fig. 2C).

In order to determine if E-cadherin is transcriptionally down-regulated in NI+AI rats, we assessed mRNA levels of *Cdh1*, which encodes E-cadherin, as well as other junction proteins in the mucosa/submucosa. Respective mRNA levels relative to 18S rRNA were calculated for *Cdh1*, *Ctnnb1*, *Cldn2*, *Cldn7*, *Cldn8*, and *Ocln*. *Cdh1* mRNA was significantly reduced in NI+AI rats compared to the other three groups ($P<0.05$) (Fig. 3A). *Ctnnb1*, *Cldn2*, *Cldn7*, and *Cldn8* were not significantly reduced in any of the treatment groups (Fig. 3B-E). *Ocln* mRNA levels in colonic mucosa/submucosa were significantly reduced in both Ctl+AI and NI+AI rats ($P<0.05$), and there was a significant decrease in *Ocln* expression in NI+AI rats compared to NI+Ctl ($P<0.05$) (Fig. 3F). In contrast, the combination of AI+AI was not able to induce a significant change in *Cdh1* mRNA levels (Fig. 3G). In addition, there was no significant change in *Ctnnb1* (Fig. 3H) or other tight junction proteins (data not shown) when exposed to AI+AI. Similar findings were demonstrated in *Ocln* expression in groups exposed to the AI, with *Ocln* mRNA levels reduced in both Ctl+AI and AI+AI rats, compared to the Ctl+Ctl group ($P<0.05$) ($P<0.05$) (Fig. 3I). These findings demonstrate that, in contrast to other junctional proteins, *Cdh1* is the only junction protein that was significantly reduced when exposed to both NI and AI. We elected to focus on *Cdh1* rather than *Ocln,* since the latter was reduced by AI alone.

MiRNA profiling prioritizes miR-155 as a mechanistic target.

To explore the molecular mechanisms underlying the reduction of *Cdh1* mRNA levels, we used miRNA microarrays to evaluate global changes in miRNA production in the colon mucosa/submucosa of 4 groups of rats: Ctl, Ctl+AI (C-T68), NI+Ctl, and NI+AI (NI-T68). The data was deposited in the GEO Repository (Accession No. GSE138770. URL: https://www.ncbi.nlm.nih.gov/geo/query/acc.cgi?acc=GSE138770). A hierarchical cluster analysis was created for all miRNAs with a signal intensity >32 (Fig. S3). A t-test was then performed comparing the control group to the NI+AI rats. Forty-five miRNA had significant changes in expression levels ($P<0.05$) and high signal intensity (>250). When compared to controls, 24 miRNAs were increased in colon mucosa/submucosa (Table 1) and 21 were decreased (Table S1, $P<0.05$). After the initial analysis, miR-155 was prioritized because of its previously noted modulation of *Cdh1* (21).

Using IPA, miR-155 cross-referenced with TargetScan human targets. Using the biomarker dataset upload, the ingenuity identifier was selected, and an overlay of the tight junction canonical pathway was implemented (data not presented). Protein Kinase C Iota (PRKCI), a target of miR-155, was also common to tight junction signaling via its inhibition of aPKC.

Confirmation of miR-155 elevation in NI+AI rats by RT-qPCR.

To validate the miRNA array data prediction studies, RT-qPCR was performed on miR-155. In the presence of NI+AI, a significant increase in miR-155 expression in colonic mucosa was noted compared to the other three groups ($P<0.05$) (Fig. 4A). No significant increase was detected for miR-155 in Ctl+AI *vs.* Ctl+Ctl or NI+Ctl rats. For comparison, we also assessed miR-155 levels in the colonic mucosa of the rats subjected to one or two rounds of AIs. There was a slight elevation in miR-155 levels in Ctl+AI or AI+AI *vs.* Ctl+Ctl or AI +Ctl rats ($P>0.1$, Fig. 4B). *TNFα* mRNA expression was significantly upregulated in both Ctl+AI and AI+AI rats compared to Ctl+Ctl and AI+Ctl rats ($P<0.05$, Fig. 4C). No significant difference was observed in AI+AI *vs.* Ctl+AI rats.

Histone hyperacetylation at the promoter of miR-155 in the colonic mucosa/submucosa of NI+AI rats.

A direct correlation often exists between the level of histone hyperacetylation and promoter activation for a given gene of interest. To elucidate the epigenetic mechanisms underlying the miR-155 upregulation in NI+AI rats, we evaluated the histone acetylation status surrounding the core promoter region of *Mir155*. ChIP-qPCR analysis was performed using antibodies against either H3K9ac or H4K12ac, and primers specific to the rat *Mir155* gene promotor (−87/+6). This revealed that both H3K9ac (Fig. 4D) and H4K12ac (Fig. 4E) were increased significantly at the *Mir155* promoter motif in NI+AI rats compared to Ctl+Ctl, Ctl +AI, and NI+Ctl groups ($P<0.05$), indicating histone hyperacetylation and chromatin relaxation. In addition, ChIP-qPCR analysis with anti-RNA polymerase II antibody confirmed that the elevation in histone acetylation was accompanied by increased RNA polymerase II at the *Mir155* promoter ($P<0.01$) (Fig. 4F), indicative of transcriptional activation. NI alone caused slight increases in H3K9ac (Fig. 4D*, P=0.09*), H4K12ac (Fig. 4E*, P=0.17*), H3K27ac, and H3K4me3 (data not shown, $P>0.05$) (22). DNA methylation on the rat *Mir155* promoter was also quantified by qMSP with no significant difference among all 4 groups (Fig. 4G). This further supports the role of acetylation driven epigenetic modifications in the NI+AI rats.

TNFα activates miR-155 by inducing histone hyperacetylation.

High levels of H_2O_2, IL-1β, TNFα, and LPS have been found in patients with IBD and we speculated that some of these factors might upregulate miR-155 by enhancing histone acetylation (23-25). To test the hypothesis, we incubated SW620 and HEK293 cells with H_2O_2 (200 μM), IL-1β (10 ng/mL), TNFα (10 ng/mL), or LPS (10 and 100 ng/mL) for 24 hours and detected miR-155 expression by RT-qPCR. We found that only TNFα significantly elevated miR-155 expression in SW620 cells (Fig. 5A). These findings suggest that proinflammatory cytokines, but not reactive oxygen species or TLR-4 agonists, are responsible for miR-155 overexpression in colonic epithelial cells. These changes in miR-155 expression were sustained from hour 3 to 24 in both cell lines when exposed to a

fixed dose of TNFα in both SW620 (Fig. 5B) and CCD 841 CoN (Fig. 5D) cell lines. In addition, there was a dose dependent response achieved in both cell lines when exposed to TNFα (Figs. 5C, 5E). No changes in miR-155 were observed in HEK293 cells (data not shown), indicating that the upregulation of miR-155 by proinflammatory cytokines is cell type-specific. To determine whether TNFα and IL-1β activate miR-155 by inducing histone acetylation surrounding the *Mir155* promoter, SW620 cells treated with TNFα or IL-1β were fixed with 1% formaldehyde and subjected to ChIP-qPCR analysis. Both H3K9ac and H4K12ac at the *Mir155* promoter were markedly enhanced by TNFα compared to the controls. No significant increase was detected for H3K9ac and H4K12ac by IL-1β (Fig. 5F, $P>0.05$). This data suggested that TNFα, which is significantly elevated in NI+AI rats (7), rather than IL-1β primarily activates *Mir155* transcription by inducing histone hyperacetylation.

MiR-155 suppresses E-cadherin and increases monolayer permeability.

In order to confirm that E-cadherin ablation disrupts cell junction and that miR-155 targets E-cadherin, we depleted E-cadherin in SW620 cells using *CDH1* siRNA and overexpressed miR-155 by transient transfection. Intercellular junctions were evaluated by monitoring the SW620 monolayer permeability. As expected, a significant increase in monolayer permeability was noted in the *CDH1* siRNA transfection group (Fig. 6A, bar graph). This was accompanied by a significant decrease in E-cadherin protein expression compared to the control siRNA group (siCtl, Fig. 6A, Western blots). A similar decrease in E-cadherin protein was replicated when the cells were transfected with miR-155, and included a concurrent, significant increase in SW620 monolayer permeability (quantified by comparing fluorescence units counted per second) compared to an miRNA negative control ($P<0.05$) (Fig. 6B). Similar results were obtained from Caco-2 cells (data not shown). To augment our findings, *in vivo* studies were performed. Ctl+Ctl and NI+AI rats were given either miR-155 inhibitor treatment or control via enema daily for one day before and six days after exposure to AI. Colonic permeability 24 hours after the last dose was assessed, and the marked increase of colonic permeability in NI+AI rats (*vs.* Ctl+Ctl rats) was significantly mitigated by the miR-155 inhibitor (Fig. 6C, bar graph). No significant difference was noted in the Ctl +Ctl group. Western blots showed that the decrease in E-cadherin protein expression was also abrogated by the miR-155 inhibitor (Fig. 6C). These findings confirm miR-155 targeting of E-cadherin, mechanistically explaining the miRNA's association with increased epithelial permeability, and the junction protein's dependence on NI+AI for diminished expression.

DISCUSSION

Early life adversity mediated through infections and other systemic stressors are independent risk factors in IBD. Investigators have previously illustrated that term birth, breast feeding for more than 12 months, and avoidance of antibiotic exposure in early life convey some protective effect in the development of IBD (26, 27). In animal models, the early life disruption of normal gut microbiota and the subsequent loss of mucosal homeostasis is thought to confer IBD risk (28). We previously investigated durable mechanisms mediating these pathogenic changes. Using a '2-hit' chemical injury model, we demonstrated that NI

induces epigenetic changes, priming the rat for an exaggerated immune response in the setting of a second, adult stressor. Through hyperacetylation of histone H4K12, NI+AI rats had sustained upregulation of IL-1β expression in colonic epithelium. This change was dependent on the presence of NI (7). Key questions remained regarding the colonic structural alterations mediated by these epigenetic changes.

A hallmark feature of IBD is the presence of clinical flares, which in part are mediated by alterations in epithelial integrity. Changes in intestinal permeability cause alterations in the normal immune response (29). In this study, utilizing epithelial permeability as a marker for a loss of junctional integrity, we demonstrated that significant and sustained changes in barrier integrity were dependent on a combination of NI, and a subsequent AI response. We also showed that these changes in epithelial permeability were accompanied by a marked decrease in the junction protein E-cadherin, in both rat colonic mucosa/sub-mucosa as well as SW620 and CCD 841 CoN epithelial monolayers.

E-cadherin mediates cell-cell interactions at adherens junctions, but is also recognized as an important immune modulator. This is particularly true in IBD, where E-cadherin driven changes in innate immunity have been implicated in disease pathogenesis. Altered localization of E-cadherin has been shown to increase susceptibility to CD (3). The proposed mechanisms are complex, but are thought to revolve around increased intestinal permeability. This includes the weakening of tight junctions leading to direct sampling of luminal enteric bacteria by dendritic cells promoting a T cell mediated immune response (15, 30, 31). In UC, genomic analysis has identified a susceptibility loci including E-cadherin (32). Mice with a tamoxifen induced E-cadherin knockout exhibited architectural changes and increased mucosal inflammation consistent with UC. These mice also had increased hematochezia and mortality compared to controls. Both outcomes were exacerbated by subsequent episodes of systemic inflammation (33).

Interestingly, we did not note a significant reduction in other junction proteins, including β-catenin, claudin 1, claudin 2, claudin 7, claudin 8, or claudin 15 despite NI or AI exposures. Occludin was decreased only when exposed to AI, independent of the presence or absence of NI. There have been varied reports of occludin expression in IBD. In a study comparing occludin and E-cadherin expression, occludin was significantly decreased in the colonic mucosa of patients with UC in areas of active disease and in histologically quiescent areas, compared to controls. E-cadherin was downregulated only in areas of active inflammation (34). In a subsequent study of occludin expression in UC and CD, there was no significant change in the luminal epithelium of IBD patients compared to controls (35). These findings suggest that further work is warranted on the mechanisms influencing occludin expression.

While there were significant decreases in *Cdh1* encoding E-cadherin in NI+AI rats, it was relatively smaller than the subsequent decrease in NI+AI protein expression. Although there was a decrease in E-cadherin transcription, this discrepancy suggests there is likely concurrent post-translational activity mediating total intact E-cadherin levels as well. One example of this is proteolysis mediated in part by matrix metalloproteinases (MMPs). MMP-1 and MMP-3 mRNA were significantly increased in actively inflamed *vs.* quiescent UC and CD mucosa (36) , and MMP-2 has been implicated in E-cadherin cleavage (37) .

Overall, our data reinforces the role of E-cadherin as a key mediator of epithelial integrity in IBD and suggests that E-cadherin is unique among its cohort of junction proteins in its susceptibility to NI-induced expression changes. Importantly, we then demonstrated several mechanisms of inflammation-dependent changes that mediate alterations in E-cadherin expression and intestinal permeability.

MicroRNA, and their role in the modulation of gene expression, represent an active area of research interest in IBD. Initially, the role of miR-155 in tight junction signaling was investigated by bioinformatics analysis utilizing IPA software. MiR-155 has previously been demonstrated to influence expression of E-cadherin by targeting RhoA (21). We investigated pathways using predicted interactions of miR-155 and tight junction signaling. Consistent with previously described results, miR-155 was predicted to interfere with tight junction integrity through increasing expression of PRKCI (8). PRKCI overexpression has been shown to functionally inhibit atypical protein kinase C (aPKC), a molecule which assists in formation and maintenance of tight junctions (38). The impact of PRCKI expression and its effect on E-cadherin in colonic cells is unclear at this time.

In the present investigation, miR-155 was significantly increased in NI+AI rats compared to Ctl+Ctl, Ctl+AI, and NI+Ctl groups. This augmentation of miR-155 expression was confirmed by RT-qPCR. Using ChIP-qPCR, we interrogated epigenetic alterations mediating the increase in miR-155, and noted increased acetylation of H3K9 and H4K12, dependent on the presence of both NI and AI. Acetylation of lysine residues of histones H3 and H4 allowed for increased RNA polymerase II binding to the *Mir155* gene promoter site, resulting in transcriptional activation. We were unable to identify any single histone modification that is responsible for the *Mir155* promoter sensitization by NI. We postulate that NI sensitizes the *Mir155* promoter by modifying a histone code, which could be massively complex, rather than a single lysine residue.

Although increased miR-155 expression has previously been shown to correspond to increased levels of TNFα, the mechanism of this was previously unknown (39, 40). Recently, we showed that the combination of NI+AI induces an augmented immune response corresponding with a marked increase in TNFα in the colonic mucosa/submucosa (7). In the present study, we found that AI alone also increased TNFα, but two rounds of AI failed to exacerbate TNFα expression. We demonstrated that hyperacetylation at the H3K9 and H4K12 could be induced by exposure to high concentration of TNFα (≥1 ng/mL, Fig 5C, E), again resulting in a significant increase in miR-155 expression. This was unique to TNFα, and not IL-1β, and was not observed with other pro-inflammatory molecules associated with IBD: H_2O_2, and LPS. In addition, the epigenetic changes in miR-155 expression by TNFα, were recapitulated in SW620 and CCD 841 CoN colonic epithelial cells, but not in HEK 293 kidney epithelial cells.

Increased TNFα levels have been noted in the mucosa of both UC and CD patients (23-25), and play a central role in IBD pathogenesis. Anti-TNFα antibody therapy has been shown to improve rates of remission in active disease in both UC and CD (41). As a result, anti-TNFα antibody therapies have been increasingly used in IBD (42). Significant changes in miR-155 expression in the setting of NI+AI, mediated at least in part by TNFα, and the specificity of

miR-155 expression in colonic epithelium provides a compelling mechanism in which miR-155 confers an important and persistent role in the pathogenesis of IBD. Corroboration of this hypothesis might come from future preclinical studies in which miR-155 has been deleted selectively in the colon.

In the present research, we expanded on miR-155 mechanisms for direct alteration in epithelial integrity, confirming that miR-155 interferes with adherens/tight junctions by targeting and decreasing E-cadherin expression. By transfecting SW620 and CCD 841 CoN cells with miR-155, a significant decrease in E-cadherin expression occurred, mimicking transfection with *CDH1* siRNA. While this relationship has been previously described in severe pancreatitis, this is the first demonstration of this interaction in an inflammatory bowel disease model (21). This was validated by an *in vivo* model where colonic permeability was significantly decreased in NI+AI rats receiving a rectally administered miR-155 inhibitor. These findings provide an explanation for our previously noted NI+AI-dependent changes in E-cadherin levels.

In summary, our findings suggest that the combination of NI and AI in rats creates a significant and sustained change in gut permeability, and that a single insult later in life cannot recapitulate the exaggerated response triggered by an initial NI episode. This supports our previous findings that multiple AI episodes do not significantly change colonic permeability in the absence of NI. We demonstrated that, unlike other junction proteins, E-cadherin levels were selectively and significantly reduced by NI+AI exposure. The changes in E-cadherin expression were mediated, at least in part, by miR-155. In addition, miR-155 expression was uniquely increased by TNFα compared to other pro-inflammatory molecules. This in total suggests that miR-155 and its interplay with colonic permeability via E-cadherin changes plays a disease-specific role in IBD pathogenesis, and is an interesting and pertinent therapeutic target for future clinical evaluation.

Supplementary Material

Refer to Web version on PubMed Central for supplementary material.

Acknowledgements:

LC Sciences (Houston, TX) performed the miRNA microarrays and helped with data deposit.

ABBREVIATIONS:

AI	adult inflammation
ChIP	chromatin immunoprecipitation
Ctl	control
IBD	inflammatory bowel disease
CD	Crohn’s diseases
UC	ulcerative colitis

Cldn	claudin
Ocln	occludin
MMP	matrix metalloproteinase
NI	neonatal inflammation
PCR	polymerase chain reaction
sE-cad	soluble E-cadherin
TNBS	2,4,6-trinitrobenzene sulfonic acid
mRNA	messenger RNA
miRNA	micro RNA
aPKC	atypical protein kinase C
PRKCI	protein kinase C iota
FITC	fluorescein isothiocyanate
IL-1β	interleukin 1 beta
TNFα	tumor necrosis factor alpha
LPS	lipopolysaccharide
qMSP	quantitative methylation-specific PCR

REFERENCES:

1. Turner JR 2009 Intestinal mucosal barrier function in health and disease. Nat Rev Immunol 9: 799–809. [PubMed: 19855405]
2. Tunggal JA, Helfrich I, Schmitz A, Schwarz H, Gunzel D, Fromm M, Kemler R, Krieg T, and Niessen CM. 2005 E-cadherin is essential for in vivo epidermal barrier function by regulating tight junctions. EMBO J 24: 1146–1156. [PubMed: 15775979]
3. Muise AM, Walters TD, Glowacka WK, Griffiths AM, Ngan BY, Lan H, Xu W, Silverberg MS, and Rotin D. 2009 Polymorphisms in E-cadherin (CDH1) result in a mis-localised cytoplasmic protein that is associated with Crohn's disease. Gut 58: 1121–1127. [PubMed: 19398441]
4. Kountouras J, Kouklakis G, Zavos C, Chatzopoulos D, Moschos J, Molyvas E, and Zavos N. 2003 Apoptosis, inflammatory bowel disease and carcinogenesis: overview of international and Greek experiences. Can J Gastroenterol 17: 249–258. [PubMed: 12704469]
5. Cepek KL, Shaw SK, Parker CM, Russell GJ, Morrow JS, Rimm DL, and Brenner MB. 1994 Adhesion between epithelial cells and T lymphocytes mediated by E-cadherin and the alpha E beta 7 integrin. Nature 372: 190–193. [PubMed: 7969453]
6. Higgins JM, Mandlebrot DA, Shaw SK, Russell GJ, Murphy EA, Chen YT, Nelson WJ, Parker CM, and Brenner MB. 1998 Direct and regulated interaction of integrin alphaEbeta7 with E-cadherin. J Cell Biol 140: 197–210. [PubMed: 9425167]
7. Zhong XS, Winston JH, Luo X, Kline KT, Nayeem SZ, Cong Y, Savidge TC, Dashwood RH, Powell DW, and Li Q. 2018 Neonatal Colonic Inflammation Epigenetically Aggravates Epithelial Inflammatory Responses to Injury in Adult Life. Cellular and molecular gastroenterology and hepatology 6: 65–78. [PubMed: 29928672]

8. Hsu SD, Lin FM, Wu WY, Liang C, Huang WC, Chan WL, Tsai WT, Chen GZ, Lee CJ, Chiu CM, Chien CH, Wu MC, Huang CY, Tsou AP, and Huang HD. 2011 miRTarBase: a database curates experimentally validated microRNA-target interactions. Nucleic Acids Res 39: D163–169. [PubMed: 21071411]

9. Paraskevi A, Theodoropoulos G, Papaconstantinou I, Mantzaris G, Nikiteas N, and Gazouli M. 2012 Circulating MicroRNA in inflammatory bowel disease. J Crohns Colitis 6: 900–904. [PubMed: 22386737]

10. Chapman CG, and Pekow J. 2015 The emerging role of miRNAs in inflammatory bowel disease: a review. Therapeutic advances in gastroenterology 8: 4–22. [PubMed: 25553076]

11. Rodriguez A, Vigorito E, Clare S, Warren MV, Couttet P, Soond DR, van Dongen S, Grocock RJ, Das PP, Miska EA, Vetrie D, Okkenhaug K, Enright AJ, Dougan G, Turner M, and Bradley A. 2007 Requirement of bic/microRNA-155 for normal immune function. Science 316: 608–611. [PubMed: 17463290]

12. Takagi T, Naito Y, Mizushima K, Hirata I, Yagi N, Tomatsuri N, Ando T, Oyamada Y, Isozaki Y, Hongo H, Uchiyama K, Handa O, Kokura S, Ichikawa H, and Yoshikawa T. 2010 Increased expression of microRNA in the inflamed colonic mucosa of patients with active ulcerative colitis. J Gastroenterol Hepatol 25 Suppl 1: S129–133. [PubMed: 20586854]

13. Oertli M, Engler DB, Kohler E, Koch M, Meyer TF, and Muller A. 2011 MicroRNA-155 is essential for the T cell-mediated control of Helicobacter pylori infection and for the induction of chronic Gastritis and Colitis. J Immunol 187: 3578–3586. [PubMed: 21880981]

14. O'Connell RM, Kahn D, Gibson WS, Round JL, Scholz RL, Chaudhuri AA, Kahn ME, Rao DS, and Baltimore D. 2010 MicroRNA-155 promotes autoimmune inflammation by enhancing inflammatory T cell development. Immunity 33: 607–619. [PubMed: 20888269]

15. Siddiqui KR, Laffont S, and Powrie F. 2010 E-cadherin marks a subset of inflammatory dendritic cells that promote T cell-mediated colitis. Immunity 32: 557–567. [PubMed: 20399121]

16. Singh R, Chandrashekharappa S, Bodduluri SR, Baby BV, Hegde B, Kotla NG, Hiwale AA, Saiyed T, Patel P, Vijay-Kumar M, Langille MGI, Douglas GM, Cheng X, Rouchka EC, Waigel SJ, Dryden GW, Alatassi H, Zhang HG, Haribabu B, Vemula PK, and Jala VR. 2019 Enhancement of the gut barrier integrity by a microbial metabolite through the Nrf2 pathway. Nat Commun 10: 89. [PubMed: 30626868]

17. Li Q, Winston JH, and Sarna SK. 2013 Developmental origins of colon smooth muscle dysfunction in IBS-like rats. Am J Physiol Gastrointest Liver Physiol 305: G503–512. [PubMed: 23886858]

18. Li Q, Winston JH, and Sarna SK. 2016 Noninflammatory upregulation of nerve growth factor underlies gastric hypersensitivity induced by neonatal colon inflammation. Am J Physiol Regul Integr Comp Physiol 310: R235–242. [PubMed: 26608656]

19. Moura J, Sorensen A, Leal EC, Svendsen R, Carvalho L, Willemoes RJ, Jorgensen PT, Jenssen H, Wengel J, Dalgaard LT, and Carvalho E. 2019 microRNA-155 inhibition restores Fibroblast Growth Factor 7 expression in diabetic skin and decreases wound inflammation. Sci Rep 9: 5836. [PubMed: 30967591]

20. Ye J, Kang Y, Sun X, Ni P, Wu M, and Lu S. 2017 MicroRNA-155 Inhibition Promoted Wound Healing in Diabetic Rats. The international journal of lower extremity wounds 16: 74–84. [PubMed: 28682732]

21. Tian R, Wang RL, Xie H, Jin W, and Yu KL. 2013 Overexpressed miRNA-155 dysregulates intestinal epithelial apical junctional complex in severe acute pancreatitis. World J Gastroenterol 19: 8282–8291. [PubMed: 24363519]

22. Igolkina AA, Zinkevich A, Karandasheva KO, Popov AA, Selifanova MV, Nikolaeva D, Tkachev V, Penzar D, Nikitin DM, and Buzdin A. 2019 H3K4me3, H3K9ac, H3K27ac, H3K27me3 and H3K9me3 Histone Tags Suggest Distinct Regulatory Evolution of Open and Condensed Chromatin Landmarks. Cells 8.

23. Masuda H, Iwai S, Tanaka T, and Hayakawa S. 1995 Expression of IL-8, TNF-alpha and IFN-gamma m-RNA in ulcerative colitis, particularly in patients with inactive phase. J Clin Lab Immunol 46: 111–123. [PubMed: 8926619]

24. Reimund JM, Wittersheim C, Dumont S, Muller CD, Kenney JS, Baumann R, Poindron P, and Duclos B. 1996 Increased production of tumour necrosis factor-alpha interleukin-1 beta, and

interleukin-6 by morphologically normal intestinal biopsies from patients with Crohn's disease. Gut 39: 684–689. [PubMed: 9026483]

25. Murch SH, Braegger CP, Walker-Smith JA, and MacDonald TT. 1993 Location of tumour necrosis factor alpha by immunohistochemistry in chronic inflammatory bowel disease. Gut 34: 1705–1709. [PubMed: 8031350]
26. Sonntag B, Stolze B, Heinecke A, Luegering A, Heidemann J, Lebiedz P, Rijcken E, Kiesel L, Domschke W, Kucharzik T, and Maaser C. 2007 Preterm birth but not mode of delivery is associated with an increased risk of developing inflammatory bowel disease later in life. Inflamm Bowel Dis 13: 1385–1390. [PubMed: 17567873]
27. Hviid A, Svanstrom H, and Frisch M. 2011 Antibiotic use and inflammatory bowel diseases in childhood. Gut 60: 49–54. [PubMed: 20966024]
28. Renz H, Brandtzaeg P, and Hornef M. 2011 The impact of perinatal immune development on mucosal homeostasis and chronic inflammation. Nat Rev Immunol 12: 9–23. [PubMed: 22158411]
29. Mankertz J, and Schulzke JD. 2007 Altered permeability in inflammatory bowel disease: pathophysiology and clinical implications. Curr Opin Gastroenterol 23: 379–383. [PubMed: 17545772]
30. Sanders DS 2005 Mucosal integrity and barrier function in the pathogenesis of early lesions in Crohn's disease. J Clin Pathol 58: 568–572. [PubMed: 15917403]
31. Jiang A, Bloom O, Ono S, Cui W, Unternaehrer J, Jiang S, Whitney JA, Connolly J, Banchereau J, and Mellman I. 2007 Disruption of E-cadherin-mediated adhesion induces a functionally distinct pathway of dendritic cell maturation. Immunity 27: 610–624. [PubMed: 17936032]
32. Barrett JC, Lee JC, Lees CW, Prescott NJ, Anderson CA, Phillips A, Wesley E, Parnell K, Zhang H, Drummond H, Nimmo ER, Massey D, Blaszczyk K, Elliott T, Cotterill L, Dallal H, Lobo AJ, Mowat C, Sanderson JD, Jewell DP, Newman WG, Edwards C, Ahmad T, Mansfield JC, Satsangi J, Parkes M, Mathew CG, Donnelly P, Peltonen L, Blackwell JM, Bramon E, Brown MA, Casas JP, Corvin A, Craddock N, Deloukas P, Duncanson A, Jankowski J, Markus HS, McCarthy MI, Palmer CN, Plomin R, Rautanen A, Sawcer SJ, Samani N, Trembath RC, Viswanathan AC, Wood N, Spencer CC, Bellenguez C, Davison D, Freeman C, Strange A, Langford C, Hunt SE, Edkins S, Gwilliam R, Blackburn H, Bumpstead SJ, Dronov S, Gillman M, Gray E, Hammond N, Jayakumar A, McCann OT, Liddle J, Perez ML, Potter SC, Ravindrarajah R, Ricketts M, Waller M, Weston P, Widaa S, Whittaker P, Attwood AP, Stephens J, Sambrook J, Ouwehand WH, McArdle WL, Ring SM, Strachan DP, U. I. G. Consortium, and W. T. C. C. C. 2. 2009 Genome-wide association study of ulcerative colitis identifies three new susceptibility loci, including the HNF4A region. Nat Genet 41: 1330–1334. [PubMed: 19915572]
33. Grill JI, Neumann J, Hiltwein F, Kolligs FT, and Schneider MR. 2015 Intestinal E-cadherin Deficiency Aggravates Dextran Sodium Sulfate-Induced Colitis. Dig Dis Sci 60: 895–902. [PubMed: 25634675]
34. Kucharzik T, Walsh SV, Chen J, Parkos CA, and Nusrat A. 2001 Neutrophil transmigration in inflammatory bowel disease is associated with differential expression of epithelial intercellular junction proteins. Am J Pathol 159: 2001–2009. [PubMed: 11733350]
35. Das P, Goswami P, Das TK, Nag T, Sreenivas V, Ahuja V, Panda SK, Gupta SD, and Makharia GK. 2012 Comparative tight junction protein expressions in colonic Crohn's disease, ulcerative colitis, and tuberculosis: a new perspective. Virchows Arch 460: 261–270. [PubMed: 22297703]
36. von Lampe B, Barthel B, Coupland SE, Riecken EO, and Rosewicz S. 2000 Differential expression of matrix metalloproteinases and their tissue inhibitors in colon mucosa of patients with inflammatory bowel disease. Gut 47: 63–73. [PubMed: 10861266]
37. Grabowska MM, and Day ML. 2012 Soluble E-cadherin: more than a symptom of disease. Frontiers in bioscience (Landmark edition) 17: 1948–1964. [PubMed: 22201848]
38. Suzuki A, and Ohno S. 2006 The PAR-aPKC system: lessons in polarity. J Cell Sci 119: 979–987. [PubMed: 16525119]
39. Tili E, Michaille JJ, Cimino A, Costinean S, Dumitru CD, Adair B, Fabbri M, Alder H, Liu CG, Calin GA, and Croce CM. 2007 Modulation of miR-155 and miR-125b levels following lipopolysaccharide/TNF-alpha stimulation and their possible roles in regulating the response to endotoxin shock. J Immunol 179: 5082–5089. [PubMed: 17911593]

40. Bala S, Marcos M, Kodys K, Csak T, Catalano D, Mandrekar P, and Szabo G. 2011 Up-regulation of microRNA-155 in macrophages contributes to increased tumor necrosis factor {alpha} (TNF{alpha}) production via increased mRNA half-life in alcoholic liver disease. J Biol Chem 286: 1436–1444. [PubMed: 21062749]

41. Ford AC, Sandborn WJ, Khan KJ, Hanauer SB, Talley NJ, and Moayyedi P. 2011 Efficacy of biological therapies in inflammatory bowel disease: systematic review and meta-analysis. Am J Gastroenterol 106: 644–659, quiz 660. [PubMed: 21407183]

42. Yu H, MacIsaac D, Wong JJ, Sellers ZM, Wren AA, Bensen R, Kin C, and Park KT. 2018 Market share and costs of biologic therapies for inflammatory bowel disease in the USA. Aliment Pharmacol Ther 47: 364–370. [PubMed: 29164650]

Key points:

- Neonatal inflammation (NI) in the colon affects barrier function later in life.
- NI sensitizes the Mir155 promoter for aberrant epigenetic activation.
- miR-155 suppresses E-cadherin protein expression in the colonic epithelium.

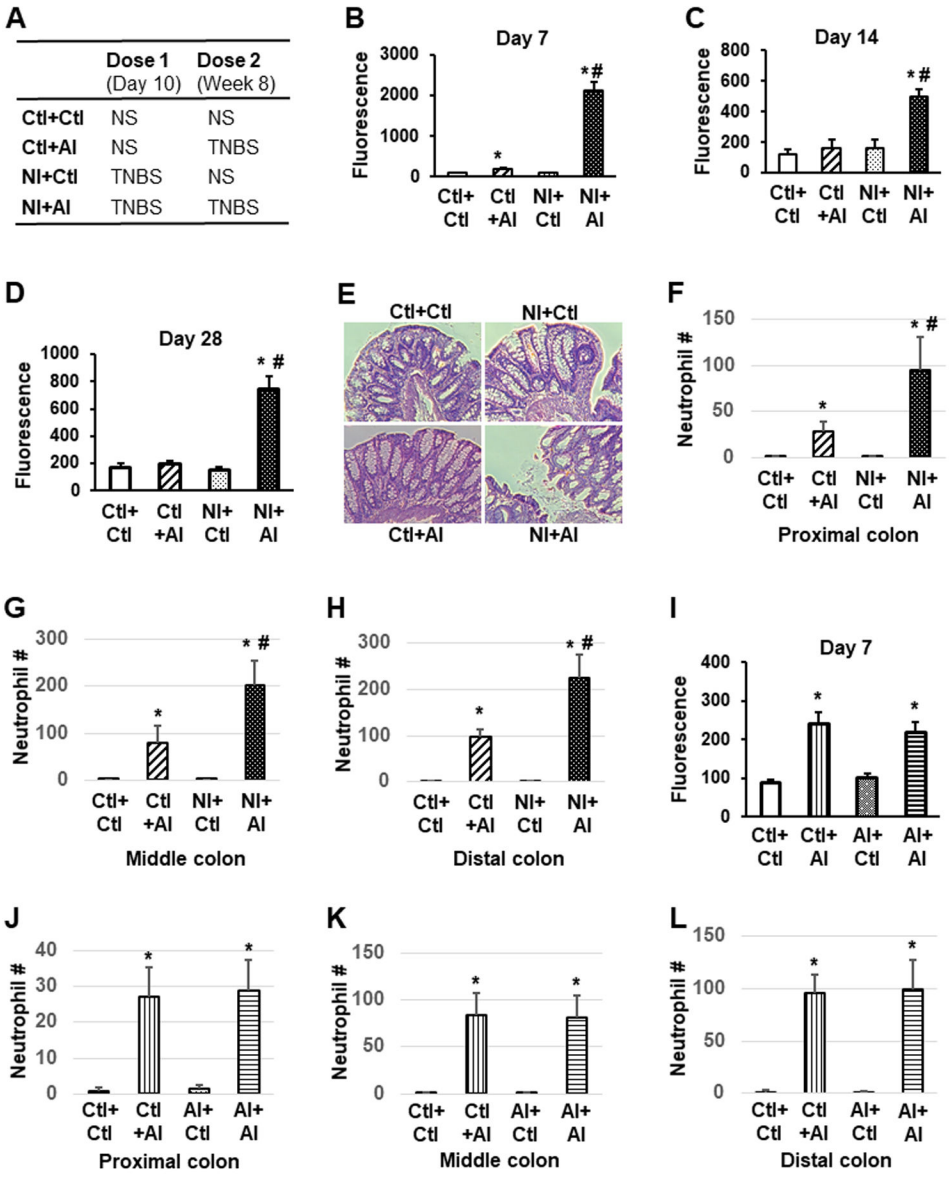

Fig. 1.

Aggravated mucosal injury in the rats subjected to both neonatal inflammation (NI) and adult inflammation (AI) in the colon. *A*: Diagram displaying the animal protocol including administration timing of TNBS and normal saline (NS). Colonic permeability in rats exposed to NI, or AI, or both, was measured using FITC-dextran at day 7 (*B*), 14 (*C*) and 28 (*D*). n=15. * $P<0.05$ *vs.* Ctl+Ctl; # $P<0.05$ *vs.* Ctl+AI. (*E*) H&E staining of the colon. Neutrophil infiltration at day 7 in proximal (*F*), middle (*G*), and distal (*H*) colon was evaluated by two independent pathologists. n=12. * $P<0.05$ *vs.* Ctl+Ctl; # $P<0.05$ *vs.* Ctl +AI. For comparison, four groups of adult rats were exposed to either one or two rounds of AI and the colonic permeability was assessed 7 days later (*I*). Neutrophils in the proximal (J), middle (K), and distal (L) colon were also examined by two independent pathologists. ANOVA. n=12. * $P<0.05$ *vs.* Ctl+Ctl.

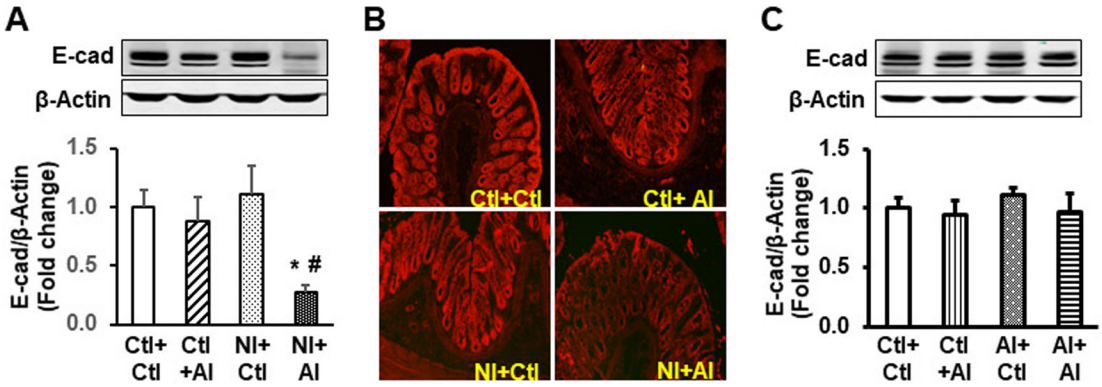

Fig. 2.

Significant suppression of E-Cadherin protein in the colonic mucosa/submucosa of NI+AI rats. *A:* E-cadherin protein levels were markedly down-regulated in the colonic mucosa/submucosa of NI+AI rats. Top: representative images of Western blots. Bottom: Arbitrary optical density units of E-cadherin (E-cad) were normalized against β-Actin and expressed as fold change. ANOVA. n=12. * $P<0.05$ *vs.* Ctl+Ctl; # $P<0.05$ *vs.* Ctl+AI. *B:* Immunofluorescence staining of E-cadherin demonstrating decreased relative intensity in the colon of NI+AI rats. *C*: Two rounds of AI had no effect on E-cadherin protein expression in the colonic mucosa/submucosa. Top: representative images of Western blots. Bottom: Arbitrary optical density units of the targeting protein were normalized *vs.* β-Actin and presented as fold change.

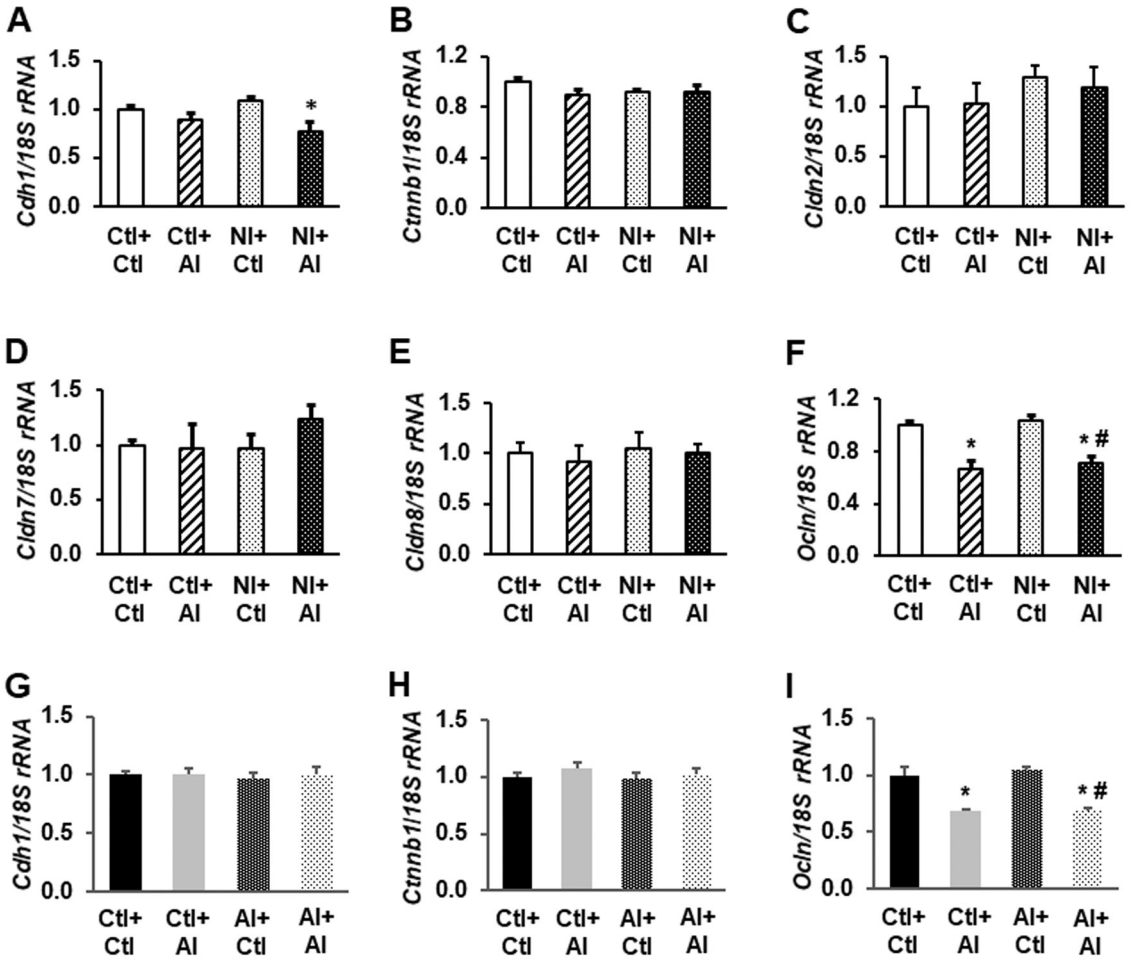

Fig. 3.

mRNA levels of junction proteins in the colonic mucosa/submucosa of 8 groups of rats. Total RNA was isolated from the colonic mucosa/submucosa. mRNA expression levels of *Cdh1* (*A*), *Ctnnb1* (*B*), *Cldn2* (*C*), *Cldn7* (*D*), *Cldn8* (*E*), and *Ocln* (*F*) in Ctl+Ctl, Ctl+AI, NI+Ctl, and NI+AI rats were quantified by TaqMan-based RT-qPCR. n=12. ANOVA. * $P<0.05$ *vs.* Ctl+Ctl. # $P<0.05$ *vs.* NI+Ctl. mRNA levels of *Cdh1* (*G*), *Ctnnb1* (*H*), and *Ocln* (*I*) in Ctl+Ctl, Ctl+AI, AI+Ctl, and AI+AI rats were also determined by RT-qPCR. n=12. * $P<0.05$ *vs.* Ctl+Ctl. # $P<0.05$ *vs.* AI+Ctl.

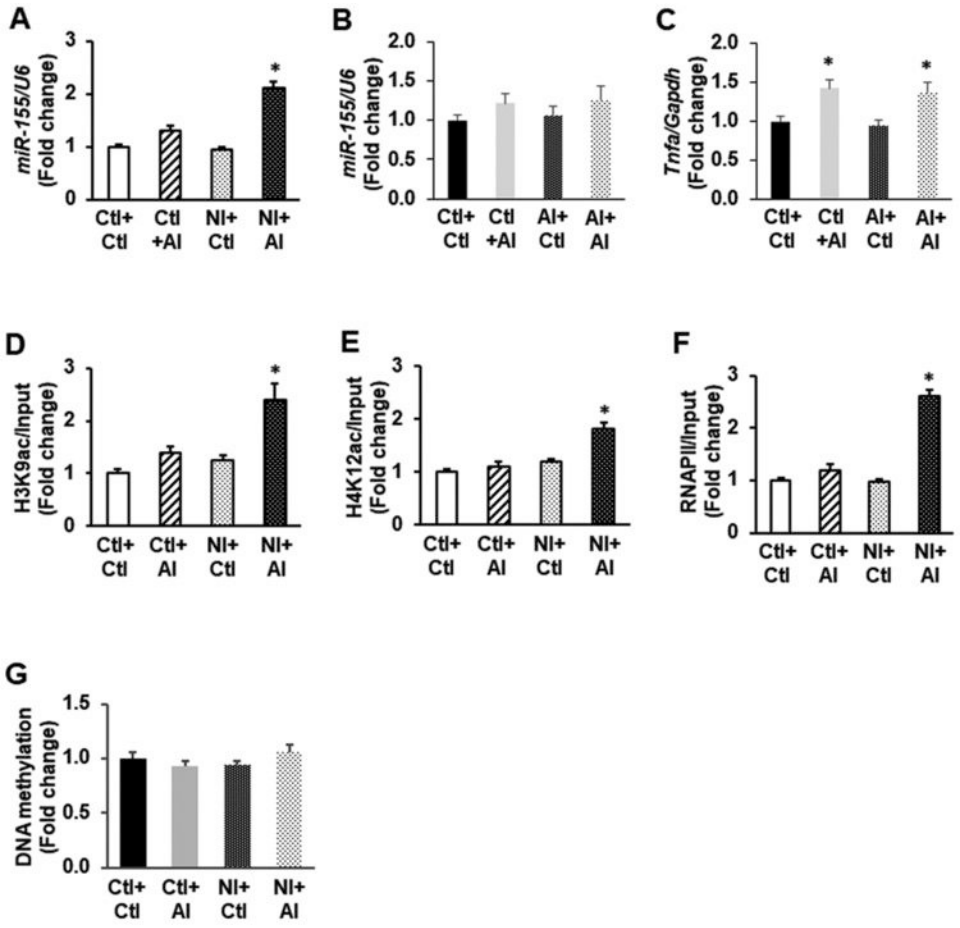

Fig. 4.

Epigenetic mechanisms underlying miR-155 elevation in NI+AI rats. *A:* RT-qPCR validation of miRNA microarray data confirming a significant increase in miR-155 expression in the colonic mucosa/submucosa of NI+AI rats. n=12. ANOVA. * $P<0.05$ *vs.* Ctl+Ctl, Ctl+AI, and NI+Ctl groups. In the colonic mucosa/submucosa of Ctl+Ctl, Ctl+AI, AI+Ctl, and AI +AI rats, miR-155 (*B*) and TNFα (*C*) levels were also quantified by RT-qPCR. n=8. * $P<0.05$ *vs.* Ctl+Ctl and AI+Ctl groups. H3K9ac (*D*), H4K12ac (*E*), and RNAPII (*F*) bound to the rat *Mir155* promoter in the colonic mucosa/submucosa of NI+AI rats were quantified by ChIP-qPCR. Chromatin immunoprecipitated with specific antibodies, as indicated, was quantified by real-time PCR using primers specific to the core promoter of the rat *Mir155* gene, and normalized to inputs. DNA methylation (*G*) on the rat *Mir155* promoter was quantified by SYBR Green-based qMSP. n=3 independent experiments. ANOVA. * $P<0.05$ *vs.* Ctl+Ctl, Ctl+AI, and NI+Ctl groups.

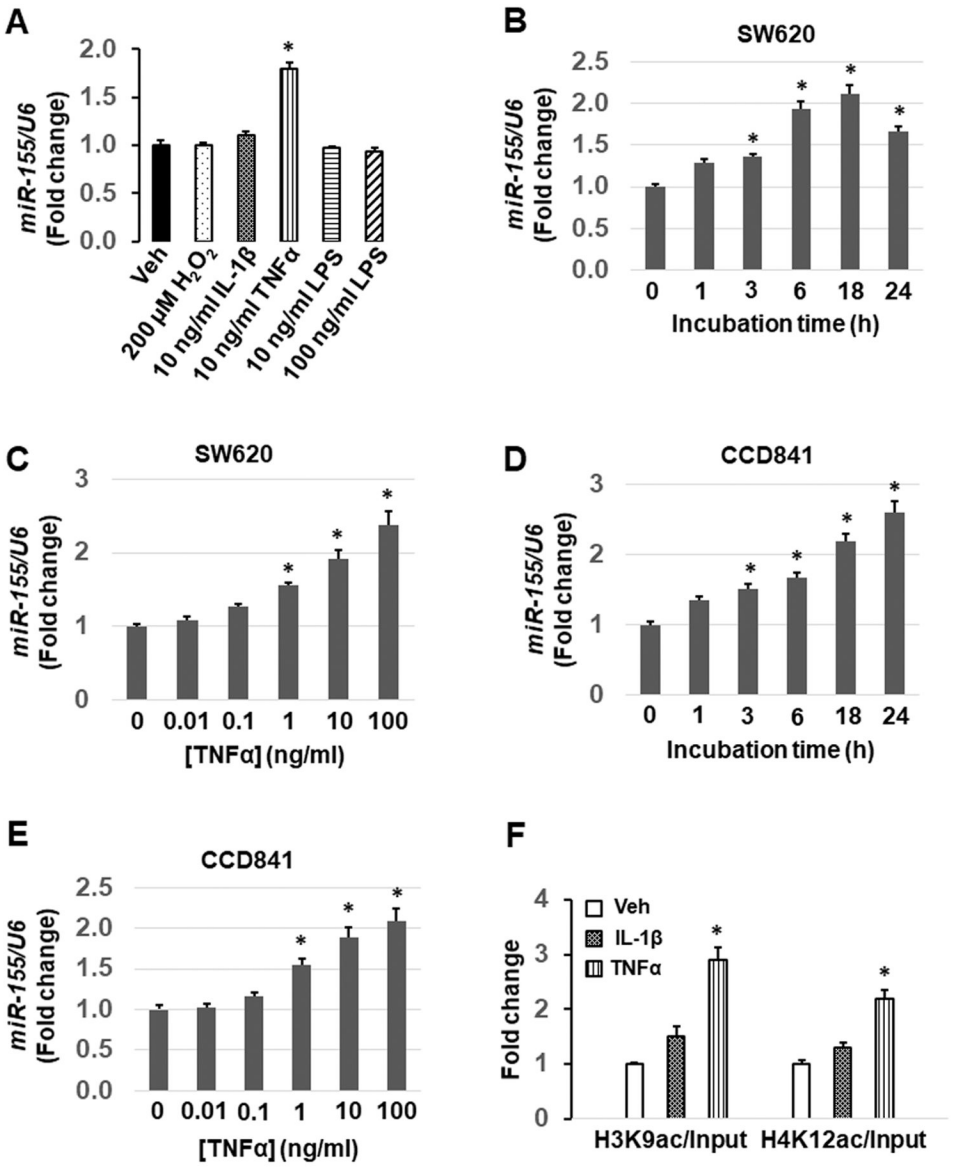

Fig. 5.

Epigenetic upregulation of miR-155 by TNFα in SW620 and CCD 841 coN colon epithelial cells. miR-155 expression levels were quantified by TaqMan Advanced miRNA Assay. *A:* TNFα significantly increased miR-155 expression compared to other known pro-inflammatory molecules and control. **P*<0.05 *vs.* vehicle-treated cells. In SW620 (*B*) and CCD 841 coN (*D*) cells, a significant increase in miR-155 expression was achieved at 3, 6, 18, and 24 hour intervals when exposed to 100 ng/ml TNFα. In addition, both SW620 (*C*) and CCD 841 coN (*E*) cell lines achieved a dose dependent increase in miR-155 expression at concentrations of 1 ng/mL of TNFα and above. **P*<0.05 compared to time "0" (time course) or concentration "0" (dose response). *F:* H3K9ac and H4K12ac surrounding the human *MIR155* promoter were evaluated by ChIP-qPCR. SW620 cells were treated with 100 ng/ml IL-1β or TNFα for 24 hours. n=3 independent experiments. T-test. * *P*<0.05 *vs.* vehicle-treated cells.

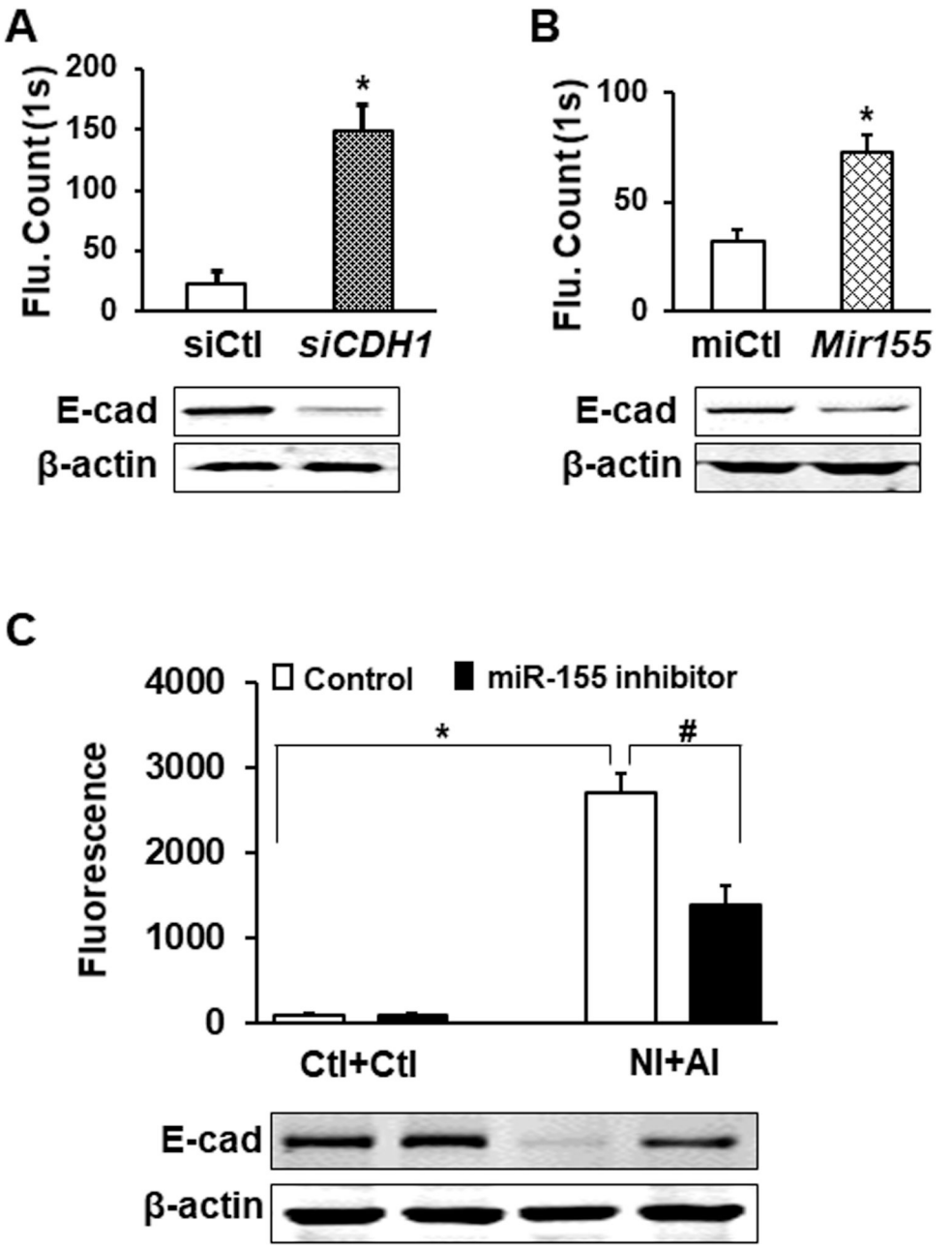

Fig. 6.

miR-155 disrupts epithelial integrity by suppressing E-cadherin. *A:* E-cadherin depletion increased SW620 monolayer permeability. *B:* miR-155 suppressed E-cadherin protein expression and increased SW620 monolayer permeability. *CDH1* siRNA and miR-155 mimics were overexpressed in SW620 cells by transient transfection. *In vitro* permeability was assessed by measuring the transport of FITC–dextran across the epithelial cell monolayer. n=5 independent experiments. T-test. * $P<0.05$. *C*: *In vivo* inhibition of miR-155 mitigated the increase of colonic permeability and the decrease of E-cadherin in NI+AI rats. Animals were treated with either control or miR-155 inhibitor via daily enema for 7 days. Colonic permeability was evaluated by measuring the transport of FITC-dextran across the

colon epithelium. ANOVA. n=8. E-cadherin (E-cad) and β-actin protein levels were detected by Western blots.

Table 1.

miRNAs increased (P<0.05) in the colon mucosa/submucosa of NI+AI rats compared to Ctl+Ctl rats.

		Ctl+Ctl	NI+AI	
miRNA Name	**p-value**	**Mean**	**Mean**	**Log2(G2/G1)**
rno-miR-139-5p	2.10E-03	1,600	3,050	0.93
rno-miR-3596c	7.45E-03	1,255	3,760	1.58
rno-miR-205	8.11E-03	4,638	6,093	0.39
rno-miR-151-3p	8.86E-03	409	604	0.56
rno-miR-3596a	9.31E-03	6,807	15,051	1.14
rno-miR-378a-5p	1.46E-02	380	700	0.88
rno-miR-196c-3p	1.59E-02	14,898	23,674	0.67
rno-miR-185-5p	1.87E-02	798	972	0.29
rno-miR-652-3p	1.88E-02	1,181	1,784	0.59
rno-miR-18a-5p	2.45E-02	256	446	0.80
rno-miR-375-3p	2.80E-02	11,682	16,083	0.46
rno-miR-345-5p	3.22E-02	202	321	0.67
rno-miR-671	3.48E-02	396	910	1.20
rno-miR-1843-3p	3.86E-02	353	1,090	1.63
rno-miR-18a-5p	4.02E-02	310	632	1.03
rno-miR-152-3p	4.23E-02	3,368	4,503	0.42
rno-miR-3596d	4.53E-02	3,552	7,521	1.08
rno-miR-378b	4.66E-02	2,633	4,013	0.61
rno-miR-155-5p	5.02E-02	273	373	0.45
rno-miR-324-5p	6.17E-02	252	429	0.77
rno-miR-1839-5p	6.85E-02	236	363	0.62
rno-miR-140-5p	8.46E-02	333	400	0.27
rno-miR-33-3p	8.63E-02	203	286	0.50
rno-miR-324-3p	8.90E-02	290	421	0.54